Kobe University Repository : Kernel

PDF issue: 2026-03-15

Enhanced metabolism of 2,3′,4,4′,5-pentachlorobiphenyl (CB118) by bacterial cytochrome P450 monooxygenase mutants of Bacillus megaterium

Ishida, Yuko ; Goto, Erika ; Haga, Yuki ; Kubo, Makoto ; Itoh, Toshimasa ; Kasai, Chie ; Tsuzuki, Harunobu ; Nakamura, Miyune ; Shoji…

(Citation)
Science of The Total Environment,890:164475

(Issue Date)
2023-09-10

(Resource Type)
journal article

(Version)
Accepted Manuscript

(Rights)
© 2023 Elsevier B.V.
This manuscript version is made available under the Creative Commons Attribution-NonCommercial-NoDerivatives 4.0 International license.

(URL)
https://hdl.handle.net/20.500.14094/0100482598

KOBE UNIVERSITY

Title: Enhanced metabolism of 2,3',4,4',5-pentachlorobiphenyl (CB118) by bacterial cytochrome P450 monooxygenase mutants of *Bacillus megaterium*

Authors: Yuko Ishida[a,#], Erika Goto[a,#], Yuki Haga[b], Makoto Kubo[c], Toshimasa Itoh[c], Chie Kasai[d], Harunobu Tsuzuki[a], Miyune Nakamura[e], Osami Shoji[d], Keiko Yamamoto[c], Chisato Matsumura[b], Takeshi Nakano[f], Hideyuki Inui[a,g,*]

[a]Graduate School of Agricultural Science, Kobe University, 1-1 Rokkodaicho, Nada-ku, Kobe, Hyogo 657-8501, Japan

[b]Hyogo Prefectural Institute of Environmental Sciences, 3-1-18 Yukihiracho, Suma-ku, Kobe, Hyogo 654-0037, Japan

[c]Laboratory of Drug Design and Medicinal Chemistry, Showa Pharmaceutical University, 3-3165 Higashi-Tamagawagakuen, Machida, Tokyo 194-8543, Japan

[d]Graduate School of Science, Nagoya University, Furo-cho, Chikusa-ku, Nagoya, Aichi, 464-8602, Japan

[e]Faculty of Agriculture, Kobe University, 1-1 Rokkodaicho, Nada-ku, Kobe, Hyogo 657-8501, Japan

[f]Research Center for Environmental Preservation, Osaka University, 2-4 Yamadaoka, Suita, Osaka 565-0871, Japan

[g]Biosignal Research Center, Kobe University, 1-1 Rokkodaicho, Nada-ku, Kobe, Hyogo 657-8501, Japan

[#]These authors contributed equally to this work.

*Corresponding Author

Hideyuki Inui, Biosignal Research Center, Kobe University, 1-1 Rokkodaicho, Nada-ku, Kobe, Hyogo, 657-8501, Japan

E-mail: hinui@kobe-u.ac.jp, Telephone number: +81-78-803-5863

Abstract

Bacterial cytochrome P450 monooxygenase P450BM3 is a promising enzyme to provide novel substrate specificity and enhanced enzymatic activity. The wild type (WT) has been shown to metabolize the widely distributed polychlorinated biphenyl (PCB) 2,3',4,4',5-pentachlorobiphenyl (CB118) to hydroxylated metabolites. However, this reaction requires the coexistence of perfluoroalkyl carboxylic acids (PFCAs). To locate P450BM3 mutants metabolizing CB118 without PFCAs, mutations were selected from amino acids comprising the substrate-binding cavity and the substrate entrance. The mutant A264G showed enhanced hydroxylation activities compared to the WT for the production of five hydroxylated metabolites. Perfluorooctanoic acid addition provided the highest activity, as found in the WT. The docking model of A264G and CB118 indicated that the enlargement of the space above the heme brought CB118 close to the heme, resulting in high activity. In contrast, the mutants L188Q, QG, LVQ, and GVQ, which contain the L188Q mutation, showed higher activity than WT even without PFCAs. Docking models revealed that the closed form found in substrate binding was induced by the L188Q mutation in the substrate non-binding state of the mutants. These mutants are promising for bioremediation of PCBs using enhanced metabolizing activities.

Keywords: docking model, hydroxylation, mutation, P450BM3, perfluoroalkyl carboxylic acid, polychlorinated biphenyl

1. Introduction

Cytochrome P450 (P450 or CYP) monooxygenases are important enzymes in most organisms for the oxidation of xenobiotics, such as pesticides and organic pollutants (Ohkawa and Inui, 2015). These reactions contribute to detoxification through the excretion of compounds to outside organisms due to increased water solubility and reduced binding affinity to toxicity-responsible receptors. For example, mammalian P450 species oxidize persistent organic pollutants such as dioxins and dioxin-like compounds (Inui et al., 2014). Dioxin-like polychlorinated biphenyls (PCBs), such as 3,3′,4,4′-tetrachlorobiphenyl (CB77), 2,3′,4,4′,5-pentachlorobiphenyl (CB118), and 3,3′,4,4′,5-pentachlorobiphenyl (CB126), are metabolized by human and rat CYP1 and CYP2 families to hydroxylated and/or dechlorinated metabolites that have less binding activity to the aryl hydrocarbon receptor (Mise et al., 2016; Yabu et al., 2022; Yamazaki et al., 2011).

PCBs are widely distributed in the environment in sea and river sediments and agricultural soil, because of their high hydrophobicity and persistence, although production of these compounds has been banned since the 1970s (Hens and Hens, 2018; Zhu et al., 2022). PCBs contaminate fish and crops through bioaccumulation, resulting in toxic effects to humans through food intake

(Weber et al., 2018). Bioremediation using microorganisms, plants, and their enzymes is a promising method to reduce PCB contamination levels (Jing et al., 2018; Khalid et al., 2021). Fungal strains reduced the concentrations of tri- to heptachlorobiphenyls (Germain et al., 2021), while bacterial consortia degrade industrial mixtures of PCBs (Horváthová et al., 2018), and enzymes related to this degradation have been isolated from PCB-degrading bacteria (Xiang et al., 2020). The P450BM3 (CYP102) from *Bacillus megaterium* that originally catalyzed hydroxylation of long-chain fatty acids, has been well studied in terms of the use of its mutants in metabolizing activities of non-substrates and the enhancement of activities toward substrates (Whitehouse et al., 2012). Its activity is high among all P450 species due to efficient electron transfer from the reductase domain located at the C-terminus of P450BM3 (Narhi and Fulco, 1987). Furthermore, P450BM3 is easily produced as a soluble protein in heterologous hosts, leading to efficient purification. These characteristics contribute to the simple crystallization of P450BM3 that allows for straightforward changes in enzymatic activities on a structural basis, resulting in a large number of P450BM3 mutants with modified activities (Whitehouse et al., 2012). Metabolic enhancement of polychlorinated dibenzo-*p*-dioxins and polycyclic aromatic hydrocarbons (PAHs) by P450BM3 mutants has been reported (Carmichael and Wong, 2001; Li et al., 2001; Sulistyaningdyah et al., 2004); however, no studies have been identified on PCB metabolism by P450BM3 or its mutants. The addition of perfluoroalkyl carboxylic acids (PFCAs)

55 to the reaction mixture enhances CB118 metabolism by P450BM3 (Goto et al., 2018). Since
56 PFCAs have similar structures to the original substrates of P450BM3, such as long-chain fatty
57 acids, P450BM3 binds to PFCAs and reacts with non-substrate compounds (Kawakami et al.,
58 2011). Although P450BM3 showed the greatest hydroxylation activity toward CB118 to produce
59 three hydroxylated metabolites, 6-hydroxy (OH)-CB118, 4′-OH-2,3′,4,5,5′-pentachlorobiphenyl
60 (4′-OH-CB120), and 3-OH-2,3′,4,4′,6-pentachlorobiphenyl (3-OH-CB119) in the presence of
61 perfluorooctanoic acid (C8), lower activities were also detected without PFCA assistance (Goto
62 et al., 2018).
63 No reports on P450BM3 mutants related to PCB metabolism been identified, although enhanced
64 metabolism of dioxins and PAHs with similar structures and physicochemical properties, such as
65 hydrophobicity, to PCBs using P450BM3 mutants have been observed (Carmichael and Wong,
66 2001; Li et al., 2001; Sulistyaningdyah et al., 2004). In this study, P450BM3 mutants that showed
67 greater metabolizing activity of CB118 than the P450BM3 wild type (WT), with and without
68 PFCAs, were selected. Furthermore, the structural bases for these metabolic pathways were
69 clarified using docking models of P450BM3 mutants to CB118. This study is useful for
70 application of the P450BM3 mutants with high PCB-metabolizing activities to bioremediation.
71

72 **2. Materials and methods**

73 2.1. Chemicals

74 CB118 (AccuStandard, New Haven, CT, USA) was dissolved in dimethyl sulfoxide (DMSO) to
75 a final concentration of 6.12 mM. PFCAs (C6 to C11, Supplementary Table 1), ^{13}C-labeled
76 hydroxylated PCBs (MHPCB-MXA: [$^{13}C_{12}$]-4-Hydroxy (OH)-3′,4′-dichlorobiphenyl, [$^{13}C_{12}$]-4-
77 OH-2′,4′,5′-trichlorobiphenyl, [$^{13}C_{12}$]-4-OH-2′,3′,4′,5′-tetrachlorobiphenyl, [$^{13}C_{12}$]-4-OH-
78 2′,3,4′,5,5′-pentachlorobiphenyl, [$^{13}C_{12}$]-4-OH-2′,3,3′,4′,5,5′-hexachlorobiphenyl, [$^{13}C_{12}$]-4-OH-
79 2,2′,3,3′,4′,5,5′-heptachlorobiphenyl, and [$^{13}C_{12}$]-4-OH-2,2′,3,4′,5,5′,6-heptachlorobiphenyl) used
80 as internal standards, and [$^{13}C_{12}$]-2,3′,4′,5-tetrachlorobiphenyl used as a syringe spike were
81 purchased from Wellington Laboratories (Guelph, Canada).

82

83 2.2. Construction of P450BM3 mutants

84 The plasmids pT7Bm3HdZ and pT7Bm3Hdz-F87A carrying P450BM3 WT and F87A mutant
85 genes were constructed as described previously (Suzuki et al., 2022). Site-directed mutagenesis
86 was conducted using primers containing the mutations (Supplementary Table 2). The primers
87 BM3 A264G-as, BM3 F87V-as, and BM3 L188Q-asM were used to construct the mutants A264G,
88 F87V, and L188Q, respectively with single mutations. The PCR conditions using KOD FX Neo
89 (Toyobo Co., Ltd., Osaka, Japan) were as follows:1 min at 95 °C, 5 min at 55 °C, and 7 min at
90 65 °C for 30 cycles after 1 min at 95 °C. After purification of the amplified plasmids using the

91 Gel/PCR DNA Isolation System (Viogene, New Taipei City, Taiwan), digestion occurred using
92 the restriction enzyme *Dpn* I. The remaining plasmids were introduced into XL10-Gold
93 Ultracompetent Cells (Agilent Technologies Japan, Ltd., Tokyo, Japan), and positive colonies
94 containing the plasmids were selected on Luria-Bertani (LB) medium containing 100 mg/L
95 ampicillin. Mutations were confirmed by sequencing using the primers BM3-s–s4, BM3-as, and
96 -as2. *Escherichia coli* strain BL21 was transformed with plasmids containing P450BM3 WT and
97 its mutant genes. The L188Q/A264G (QG, two mutations of leucine [L] at 188th and alanine [A]
98 at 264th amino acids of P450BM3 WT to glutamine [Q] and glycine [G], respectively) mutant
99 gene was constructed from L188Q by introducing the A264G mutation. The R47L/F87V/L188Q
100 (LVQ, three mutations of arginine [R] at 47th, phenylalanine [F] at 87th, and L at 188th amino acids
101 of P450BM3 WT to L, valine [V], and Q, respectively) and A74G/F87V/L188Q (GVQ, three
102 mutations of A at 74th, F at 87th, and L at 188th amino acids of P450BM3 WT to G, V, and Q,
103 respectively) mutant genes were constructed from F87V by introducing R47L and A74G,
104 respectively, followed by L188Q.
105
106 2.3. Purification of P450BM3 WT and its mutants
107 The P450BM3 WT and its mutants were produced in recombinant *E. coli* with plasmids
108 containing the corresponding genes, and purified by column chromatography according to a

109 previous study (Goto et al., 2018). Briefly, recombinant *E. coli* was incubated in liquid LB
110 medium, after which the cells were collected and sonicated to release P450BM3 and its mutants.
111 After centrifugation, the supernatants were applied to an open column containing 50 mL of
112 Celfine A-500 (Toyobo Co., Ltd., Osaka, Japan), and the samples were eluted. The red-brown
113 fractions were filtered through a Centricon filter (Amicon-Ultra, Merck Japan, Tokyo, Japan). The
114 remaining solutions were filtered using a syringe equipped with a Millex-filter unit (33 mm
115 diameter, 0.22 μm pore size, Merck Japan), and the filtrates were subjected to anion exchange
116 chromatography with TOSOH DEAE650S (Tosoh Corp., Tokyo, Japan). The elution procedure
117 was performed according to a previous study, with a slight modification (Goto et al., 2018). The
118 concentration of KCl was 0% at 0–30 min, 8% at 30–70 min, 15% at 70–160 min, 15% at 160–
119 190 min, and 100% at 190–210 min for P450BM3 WT and the five mutants. The program for QG
120 and L188Q was changed from 8 to 6%. The fractions (5 mL) were concentrated using Centricon
121 and subjected to gel filtration chromatography with TOSOH Sephacryl S200 (Tosoh). After re-
122 concentrating with Centricon, concentrations of the purified P450BM3 and its mutants were
123 determined using reduced CO difference spectra (Omura and Sato, 1964).
124
125 2.4. Metabolism of CB118 with PFCAs by P450BM3 and its mutants
126 CB118 (6.12 μM) at a final concentration of 0.1% DMSO (v/v) was reacted with 1 μM P450BM3,

100 μM PFCAs, 200 mM Tris-HCl (pH 7.4), and 5 mM NADPH in 0.5 mL reaction mixture. The reaction was initiated by adding NADPH and the mixture was incubated at 37 °C for 3 h with shaking. The controls contained the same reaction mixture without the NADPH and/or P450BM3. The reaction was stopped on ice and 20 μL of 50 ng/mL ^{13}C-labeled OH-PCBs was added. The extraction and derivatization procedures for the metabolites were the same as those described in a previous report (Goto et al., 2018). A syringe spike of 10 μL of 100 ng/mL [$^{13}C_{12}$]-2,3′,4′,5-tetrachlorobiphenyl was added. The metabolites were identified and quantified using gas chromatography and high-resolution mass spectrometry [GC/HRMS, GC, 6890N (Agilent Technologies, Tokyo, Japan); MS, JMS-800D (JEOL Ltd., Tokyo, Japan)]. The GC/HRMS conditions are presented in Supplementary Table 3.

2.5. Docking models

The docking models were constructed using the Mutate Monomers of SYBYL-X1.3 (Tripos, St Louis, MO, USA) as described previously (Ruppert et al., 1997). Docking models of P450BM3 and PFCAs (C6, C8) were constructed using the structure of P450BM3 (PDB:1FAG) with palmitoleic acid as a template. The models with CB118 were then constructed by binding CB118 to these 3D models.

145 **3. Results and discussion**

146

147 3.1. Purification of P450BM3 WT and its mutants

148 To improve hydroxylation of CB118, seven mutants (F87A, F87V, L188Q, A264G, QG, LVQ,
149 and GVQ) were constructed by site-directed mutagenesis. These amino acids are related to
150 increase metabolizing activities, not specific to PCB metabolism, by different mechanisms: the
151 amino acids F87 and A264 are in close proximity to heme, and A74 in GVQ and L188 constitute
152 the entrance of the substrate access channel (Carmichael and Wong, 2001). Mutations F87A, F87V,
153 and A264G appropriately enlarged the space above the heme because the mutated amino acids
154 are smaller than the originals. In contrast, R47 in LVQ is related to the anchoring of a substrate
155 through the carboxyl group of fatty acids (Li and Poulos, 1997). Therefore, mutations in these
156 amino acids stimulate hydroxylation of CB118. The concentrations of WT and its mutants,
157 purified from recombinant *E. coli* expressing the corresponding genes using column
158 chromatography, were calculated from the reduced CO-difference spectra. The concentrations of
159 WT, F87A, F87V, L188Q, A264G, QG, LVQ, and GVQ were 362.6, 403.8, 98.90, 140.1, 568.1,
160 321.4, 107.1, and 206.0 pmol/μL, respectively (Supplementary Figure 1).

161

162 3.2. Detections of CB118 metabolites produced by P450BM3 WT and its mutants using

163 GC/HRMS

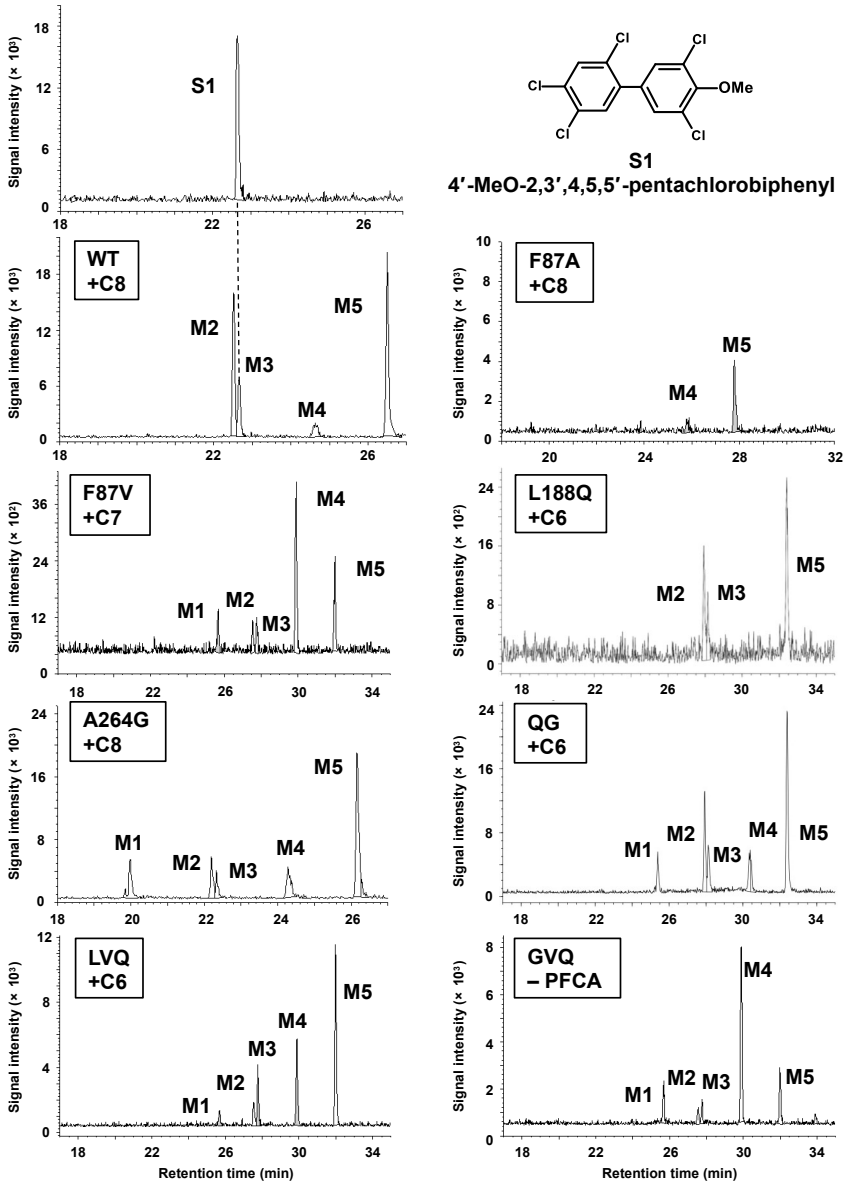

164 **Figure 1** Chromatograms of mono-hydroxylated pentachloro metabolites produced from
165 2,3′,4,4′,5-pentachlorobiphenyl (CB118) with perfluoroalkyl carboxylic acids (PFCAs) by the
166 P450BM3 wild type (WT) and its mutants by gas chromatography/high-resolution mass
167 spectrometry

168 The P450BM3 WT and its mutants, F87A, F87V, L188Q, A264G, QG (L188Q/A264G), LVQ
169 (R47L/F87V/L188Q), and GVQ(A74G/F87V/L188Q), were reacted with CB118 in the presence
170 of PFCAs. Perfluorohexanoic acid, perfluoroheptanoic acid, and perfluorooctanoic acid are

171 denoted as C6, C7, and C8, respectively. S1 is an authentic standard, 4′-methoxy-2,3′,4,5,5′-
172 pentachlorobiphenyl. Metabolites (Ms) 1–5 are described in Figure 8.

173 Two to five peaks (M1–M5) were detected in the reactions of CB118 with WT or its mutants in
174 the presence of NADPH (Figure 1). No peaks were observed in reactions without NADPH or
175 P450BM3 (Supplementary Figure 2). CB118 metabolism by P450BM3 WT and its mutants was
176 confirmed. Each peak had a similar retention time index among the P450BM3s (Supplementary
177 Table 4). As a representative, the isotope ratios of the five metabolites in A264G were analyzed
178 (Supplementary Figure 3A and 3B), and the ratios of M1–M5 and the standard S1 were similar to
179 theoretical ratios (Supplementary Table 5). These results suggest that the detected peaks were
180 derived from hydroxylated pentachloro metabolites.

181 WT, F87A, and L188Q produced four, two, and three metabolites, respectively, whereas F87V,
182 A264G, QG, LVQ, and GVQ produced five metabolites (Figures 1 and 2). M3 was identified as
183 4′-OH-CB120 because of its consistency with the retention time index of methylated 4′-OH-
184 CB120 (Supplementary Table 4). Other metabolites were not identified because their retention
185 time indices were not consistent with those of other standards. Although a previous study detected
186 three metabolites, M1, M2, and M3, these metabolites are consistent with the metabolites M2,
187 M3, and M5 named in this study (Goto et al., 2018), which indicates that M1 was newly produced
188 by the mutants.

189

3.3. Hydroxylation activities of P450BM3 WT and its mutants toward CB118 under PFCAs with

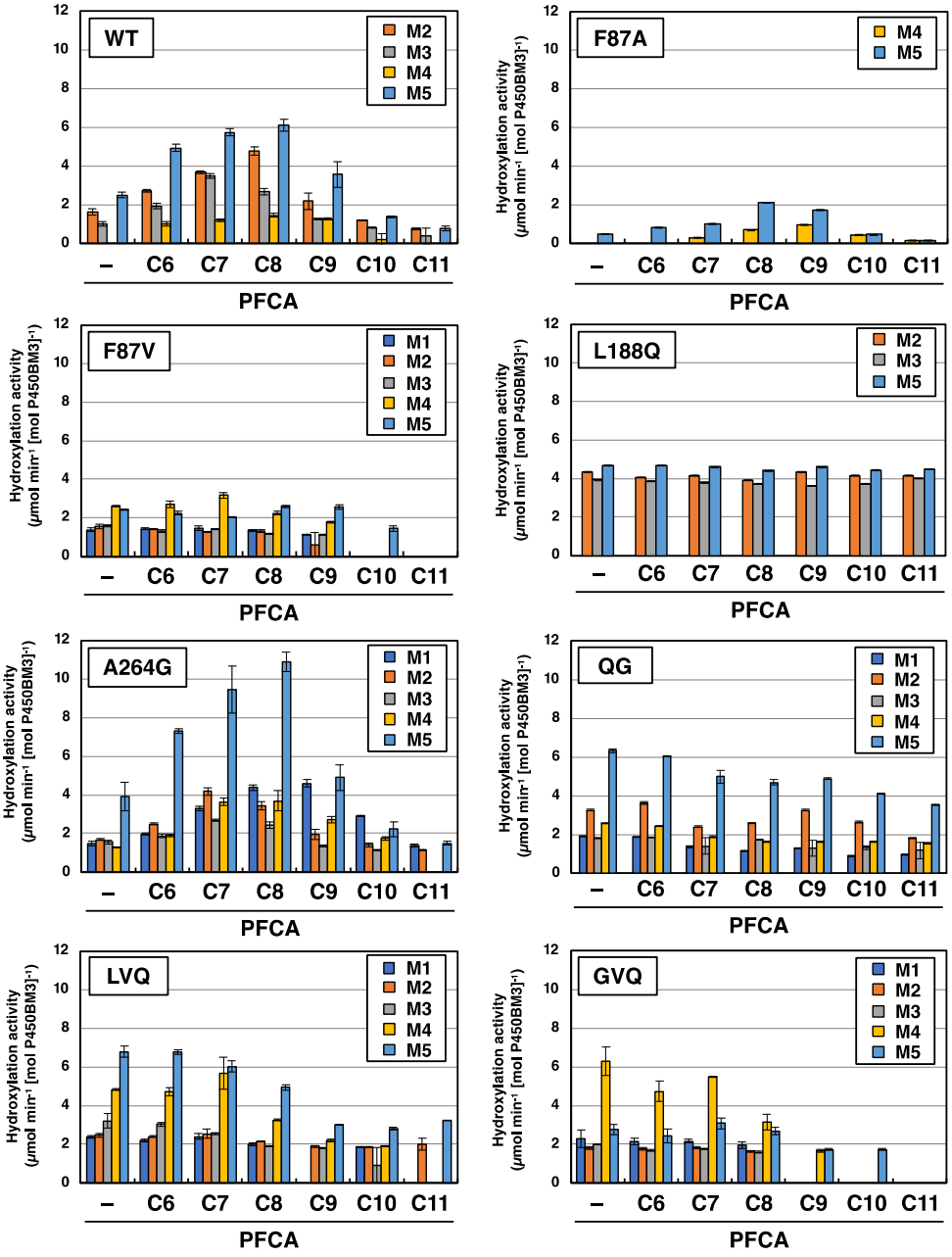

different chain lengths

Figure 2 Hydroxylation activities of the P450BM3 wild type (WT) and its mutants toward 2,3′,4,4′,5-pentachlorobiphenyl (CB118) with perfluoroalkyl carboxylic acids (PFCAs)

The P450BM3 WT and its mutants reacted with CB118 in the presence of PFCAs with carbon chain lengths of 6–11 (C6–C11). The QG, LVQ, and GVQ mutants contained the L188Q/A264G,

196 R47L/F87V/L188Q, and A74G/F87V/L188Q mutations, respectively. Error bars represent the
197 standard deviation (n = 4). Metabolites (Ms) 1–5 are described in Figure 8.

198 3.3.1. P450BM3 WT

199 The WT showed the highest total hydroxylation activity toward CB118 using C8 (Figures 2 and
200 3). Under these conditions, M5 was the most produced metabolite. The total hydroxylation
201 activity increased gradually with PFCA chain length up to C8 and decreased when approaching
202 C11. These results are consistent with those of previous studies (Goto et al., 2018). In addition,
203 C8 has been the reported as is the most suitable PFCA to accommodate CB118 in the heme in the
204 WT substrate-binding cavity (Goto et al., 2018). The metabolite M4 was newly detected in this
205 study.

206 3.3.2. P450BM3 F87A mutant

207 The F87A mutant has previously shown improved metabolism of PAHs such as phenanthrene,
208 pyrene, and fluoranthene over the WT (Carmichael and Wong, 2001). Therefore, CB118 is likely
209 also better metabolized by the F87A mutant than the WT because of the similarity of its basic
210 structure. However, the F87A mutant showed a much lower activity and number of metabolites
211 than the WT (Figures 2 and 3A). The F87A mutation appears to enlarge the substrate-binding
212 cavity near the heme to an extent that is too large to accommodate CB118 stably (Figure 4A and
213 Supplementary Figure 4). When C8 was used, the F87A mutant showed the highest total
214 hydroxylation activity toward CB118, and M5 showed greater production than M4 (Figure 2).

The pattern of total hydroxylation activities was similar to that of the WT, whereby PFCAs with

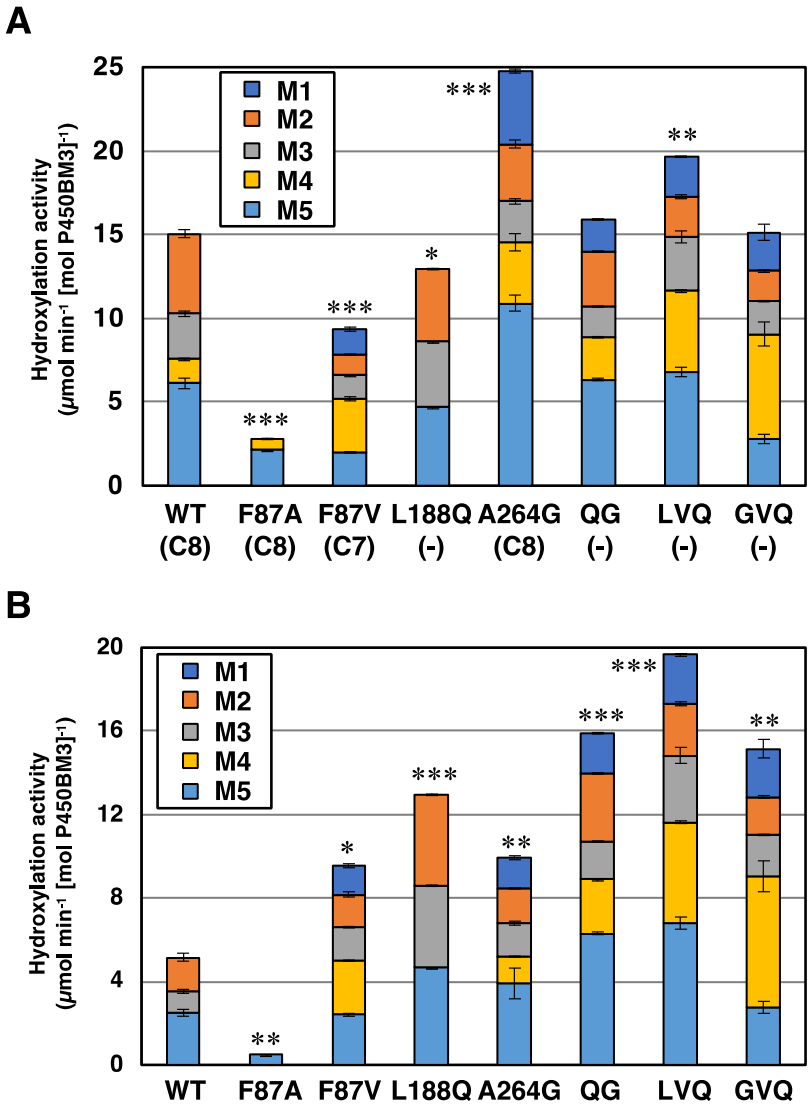

carbon chains shorter and longer than C8 caused lower activities.

Figure 3 Total hydroxylation activities of the P450BM3 wild type (WT) and its mutants toward 2,3′,4,4′,5-pentachlorobiphenyl (CB118)

Hydroxylation activities are shown when total hydroxylation activities toward all metabolites were the highest (A). The chain lengths of perfluoroalkyl carboxylic acids (PFCAs) are indicated in parentheses when the total hydroxylation activities were the highest. Total hydroxylation activities are shown without PFCAs added to the reaction mixtures (B). The QG, LVQ, and GVQ mutants contained the L188Q/A264G, R47L/F87V/L188Q, and A74G/F87V/L188Q mutations,

respectively. Error bars represent the standard deviation (n = 4). Asterisks indicate significant differences compared to the total activities of WT (*, $p < 0.05$; **, $p < 0.01$; ***, $p < 0.001$; Student's t-test). -, without PFCAs. Metabolites (Ms) 1–5 are described in Figure 8.

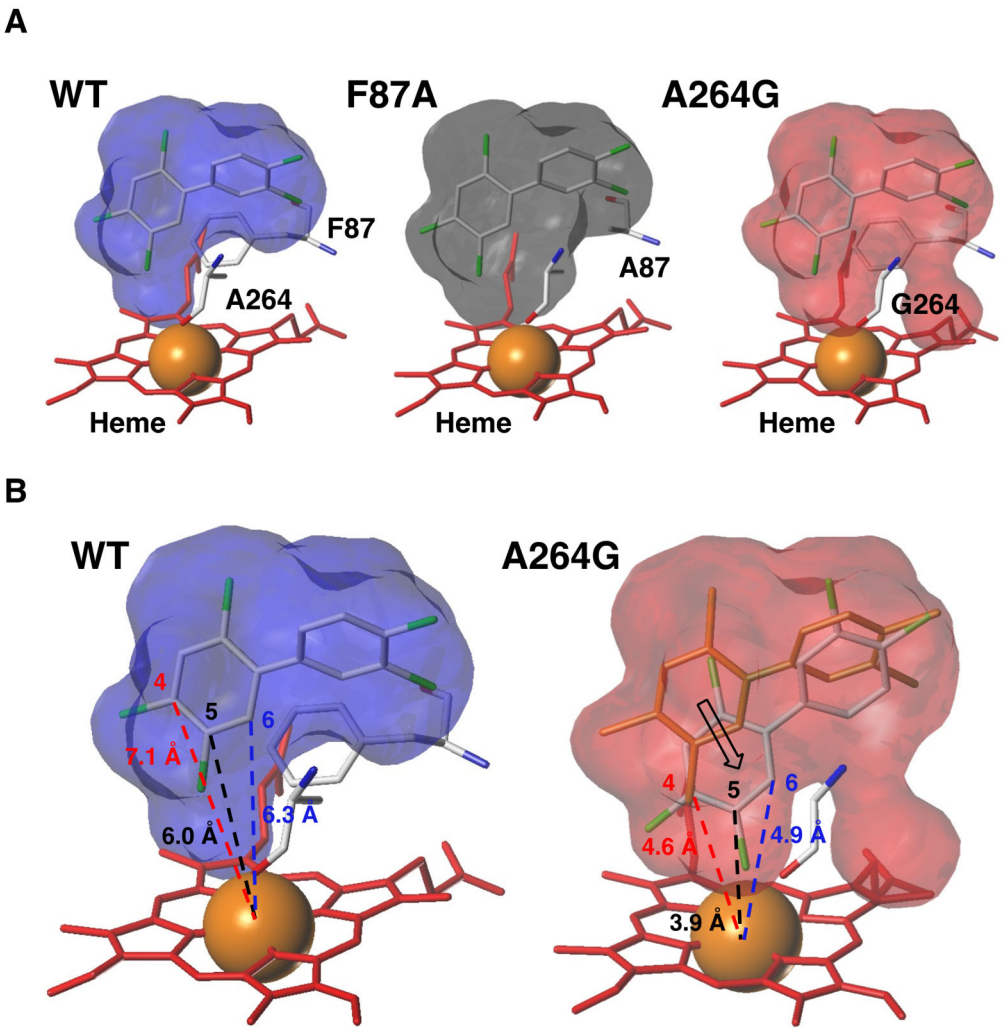

Figure 4 Docking models of the P450BM3 wild type (WT) and its mutants toward 2,3′,4,4′,5-pentachlorobiphenyl (CB118) with perfluorooctanoic acid

(A) The amino residues F87 and A264 comprise the substrate-binding cavity of P450BM3 WT. The mutations of F87A and A264G enlarge the substrate-binding cavity. The docked positions of CB118 in the mutants F87A and A264G equal those of the WT. (B) The distance between the 4-, 5-, and 6-positions of CB118, and the heme are described in red, black, and blue, respectively. In the A264G mutant, the stable position of CB118 in the cavity is moved to vicinity of the heme, as described by the arrow.

236 3.3.3. P450BM3 F87V mutant

237 The F87V mutant hydroxylated PAHs, such as naphthalene, fluorene, acenaphthene,
238 acenaphthylene, and 9-methylanthracene, with much higher activity than the WT (Li et al., 2001).
239 The addition of C7 maximized the total hydroxylation activities, and M4 showed greater
240 production that that of the other metabolites (Figure 2). No clear pattern of activity in the WT and
241 F87A was observed, whereas PFCAs with longer chains displayed decreased activity. The highest
242 total hydroxylation activity in F87V was lower than that in the WT (Figure 3A). This may be
243 caused by the unstable accommodation of CB118 in the enlarged substrate-binding cavity by the
244 mutation of F87 to valine, which is smaller than phenylalanine (Supplementary Figure 4).

245 3.3.4. P450BM3 L188Q mutant

246 P450BM3 has open and closed forms, which are substrate-free and substrate-bound states,
247 respectively (Dubey et al., 2016). The Q188 in L188Q interacts with Q73 to form a closed form,
248 resulting in CB118 metabolism without PFCA binding (Figure 5A). The L188Q mutant showed
249 the highest total hydroxylation activity without PFCAs, and M5 as the dominant metabolite
250 (Figure 2). The total hydroxylation activity in L188Q was slightly lower than that in the WT, and
251 the pattern of hydroxylation activities of the WT, F87A, and F87V, depending on the chain length
252 of PFCAs, was lost. The L188 in the WT is located at the entrance of the substrate-binding cavity
253 (Carmichael and Wong, 2001), and L188Q pushes PFCAs into the bottom of the cavity, leading

to steric hindrance against the 2- and 4-positions of CB118 (Figure 5B). Since there were no changes in hydroxylation activity depending on the length of the added PFCAs, PFCAs may be unrelated to these reactions.

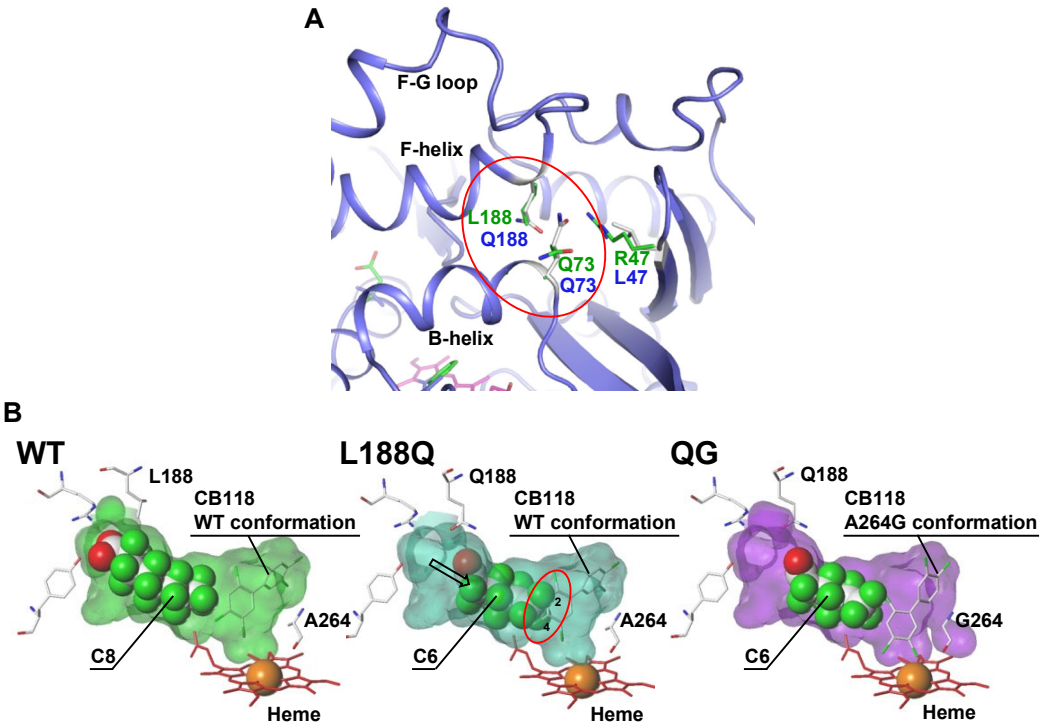

Figure 5 Docking models of the P450BM3 wild type (WT) and its mutants L188Q and L188Q/A264G (QG) toward 2,3′,4,4′,5-pentachlorobiphenyl (CB118) with perfluorohexanoic acid (C6) and perfluorooctanoic acid (C8)
Superimposed crystal structures of the WT (Protein Data Bank [PDB] ID: 1FAG) and M05 mutant (PDB ID: 4ZF6) are shown (A). Green and white sticks in amino acids were derived from WT and M05 mutants, respectively. The red circle indicates proximity and interaction between Q188 and Q73. Docking models of WT, L188Q, and QG with C6, C8, and CB118 were constructed (B). The arrow indicates movement of the carboxylic acid fixation point in the perfluoroalkyl carboxylic acid in the substrate-binding cavity of L188Q. The red circle indicates steric hindrance between C6 and CB118 in the substrate-binding cavity of L188Q.

3.3.5. P450BM3 A264G mutant

Similar to F87A, the A264G mutant shows hydroxylation activities toward PAHs (Carmichael

269 and Wong, 2001). With the addition of C8, the total hydroxylation activities were the highest
270 among the WT and other mutants (Figure 3A). M5 production was greater than that of the other
271 metabolites, and the pattern of total hydroxylation activities was similar to that of the WT and
272 F87A (Figure 2). The A264G mutation expanded the substrate-binding cavity, leading to a close
273 conformation of CB118 to the heme (Figure 4). The short distance between PCBs and P450 heme
274 results in high reaction activities (Mise et al., 2016; Yabu et al., 2022; Yamazaki et al., 2011).
275 Therefore, A264G appeared to show higher total activity than the WT.
276 3.3.6. P450BM3 QG mutant
277 The QG mutant showed a novel pattern of total hydroxylation activities, as described above, and
278 the highest activities occurred with no PCFA addition (Figure 2). The QG showed higher activities
279 than L188Q because the steric hindrance between PFCAs and CB118 was mitigated by the
280 enlargement of the substrate-binding cavity (Figure 5B). The total hydroxylation activity in QG
281 was similar to that of the WT (Figure 3A). M5 was the dominant metabolite under all conditions
282 using different chain lengths of PFCAs.
283 3.3.7. P450BM3 LVQ mutant
284 The LVQ mutant showed a similar pattern of total hydroxylation activity as QG (Figure 2). The
285 highest total hydroxylation activity was observed without PFCAs, and these activities were
286 greater than those in the WT (Figure 3A). M5 was dominantly produced under all conditions, but

its amount gradually decreased with the lengthening carbon chain of PFCAs. The P450BM3 mutants M05 and M11, which contain R47L, F87V, and L188Q, showed a closed form that is available to metabolize substrates (Supplementary Figure 5) (Geronimo et al., 2018). Therefore, LVQ likely also creates a closed form even without a substrate, leading to high hydroxylation

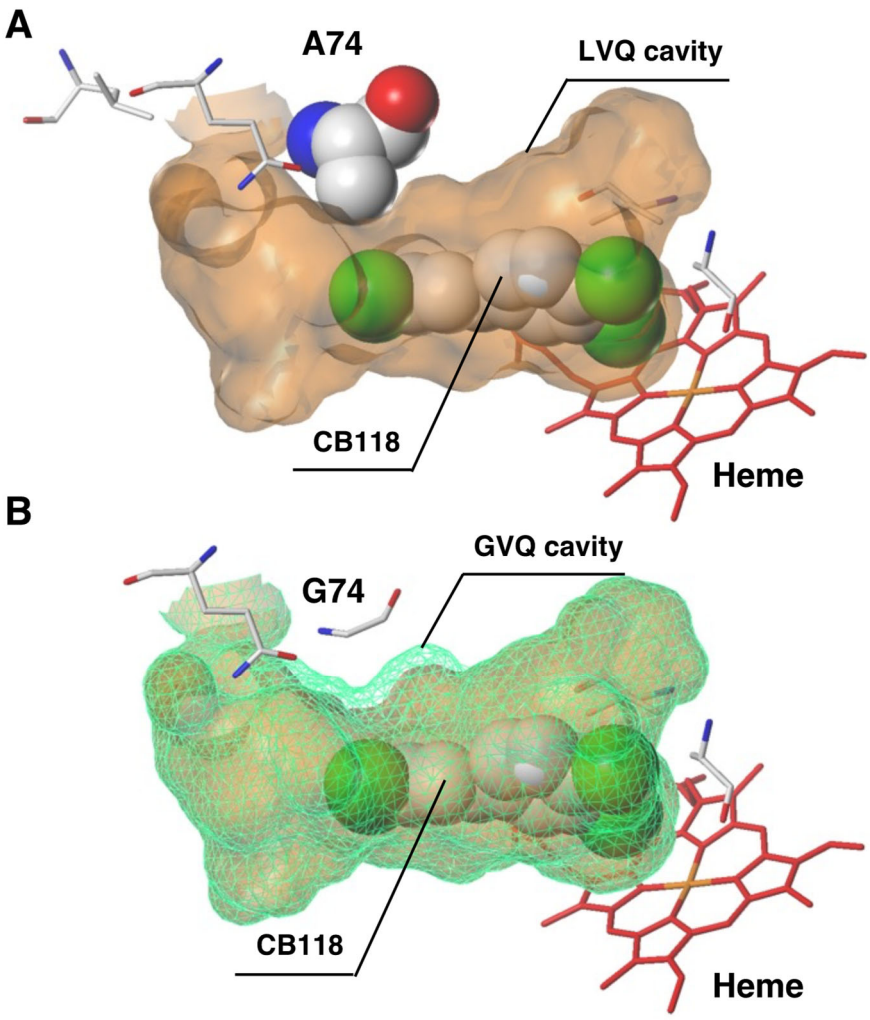

activities without PFCAs (Figure 2). In addition, this form confers different conformations of CB118 as the WT in the substrate-binding cavity (Figure 6).

Figure 6 Docking models of P450BM3 mutants toward 2,3′,4,4′,5-pentachlorobiphenyl (CB118) without perfluoroalkyl carboxylic acids

295 The LVQ and GVQ mutants contained the R47L/F87V/L188Q and A74G/F87V/L188Q
296 mutations, respectively. The substrate-binding cavity of LVQ is shown in orange (A). The
297 substrate-binding cavity of GVQ is overlaid by a green mesh (B).

298 3.3.8. P450BM3 GVQ mutant

299 The GVQ mutant hydroxylated several PAHs with higher activity than the WT and F87V (Li et
300 al., 2001). Furthermore, GVQ showed higher hydroxylation activities toward mono-, di-, and
301 trichloro dibenzo-*p*-dioxin than the WT (Sulistyaningdyah et al., 2004). The total activity in the
302 GVQ was greater than that in the WT when PFCAs were absent (Figure 3B). The pattern of total
303 hydroxylation activities in GVQ was similar to that of QG and LVQ, but the dominant metabolite
304 was M4 (Figure 2). It was also derived from the formation of a closed form due to the L188Q
305 mutation. The substrate-binding cavity of GVQ was larger than that of LVQ because G74 in GVQ
306 was smaller than A74 in LVQ (Figure 6B). These features may accommodate the bulky trichloro
307 ring of CB118 on the far side of the heme, resulting in the proximity of the dichloro ring of CB118
308 to the heme. This causes hydroxylation of the dichloro ring to produce M4.

309

310 3.4. Hydroxylation activities of P450BM3 WT and its mutants toward CB118 without PFCAs

311 The highest total hydroxylation activities are shown in Figure 3A. The F87A mutant showed
312 considerably lower activity than the WT, while the A264G and LVQ mutants exhibited higher
313 activities than the WT. These results indicate that mutations in amino acids surrounding the
314 substrate-binding cavity and existing at the entrance of the cavity increased CB118 hydroxylation

315 activities. The total hydroxylation activity in the absence of PFCAs indicated the ability of CB118
316 to metabolize without stimulation by PFCAs (Figure 3B). The mutants, except for F87A, showed
317 two to four times higher activity than the WT. The L188Q mutation inducing the closed form is
318 an important factor in ensuring a state that is prepared for the reactions, even without substrate
319 binding.
320
321 3.5. Estimation of metabolite structures from docking models and proposed metabolic pathways
322 of CB118 by P450BM3
323 The pattern of fragment ions was determined to estimate the positions of CB118 hydroxylated by
324 P450BM3 (Supplementary Figure 3C and 3D). Standard S1 showed a higher peak in the
325 chromatogram of $[M\text{-}COCH_3Cl]^+$, indicating that S1 has a hydroxyl group at *meta*- or *para*-
326 position (Supplementary Figure 3C) (Kunisue and Tanabe, 2009). Similarly, metabolites M3 and
327 M5 have a hydroxyl group at the *meta*- or *para*-position (Supplementary Figure 3D). In contrast,
328 M1, M2, and M4 revealed higher peaks in the chromatogram of $[M\text{-}CH_3Cl]^+$, indicating that these
329 metabolites have hydroxyl groups at the *ortho*-position. In a previous study, M3 was identified as
330 4′-OH-CB120, and M2 and M5 were estimated to be 6-OH-CB118 and 3-OH-CB119,
331 respectively (Figure 7B and 7C) (Goto et al., 2018). Greater productions of M2 and M5 were
332 observed by the WT than those of M3 and M4, indicating that a trichloro ring was stably

accommodated in the cavity near the heme, which is larger than those far from the heme (described as big and small cavities in the previous study) (Goto et al., 2018). The small amount of M4 produced may be due to an unstable conformation in the substrate-binding cavity or the far distance from the heme (Figure 7D). In this conformation, the 6′-position of the dichloro ring is nearest to the heme iron, resulting in the production of 6′-OH-CB118. In contrast, metabolite M1 was not produced by the WT under any of the conditions (Figure 2). It is suggested that the conformation of CB118 to produce M1 is difficult to stabilize because of the steric hindrance of the 4- and 5-positions of the trichloro ring to C8 and that of the 2-position to A264 (Figure 7A). The expansion of the cavity by the A264G mutation leads to the production of M1 by accessing the 2-position to the heme. The structure estimation was supported by the determination of the hydroxylation positions (Supplementary Figure 3D). The proposed metabolic pathways of CB118 are shown in Figure 8.

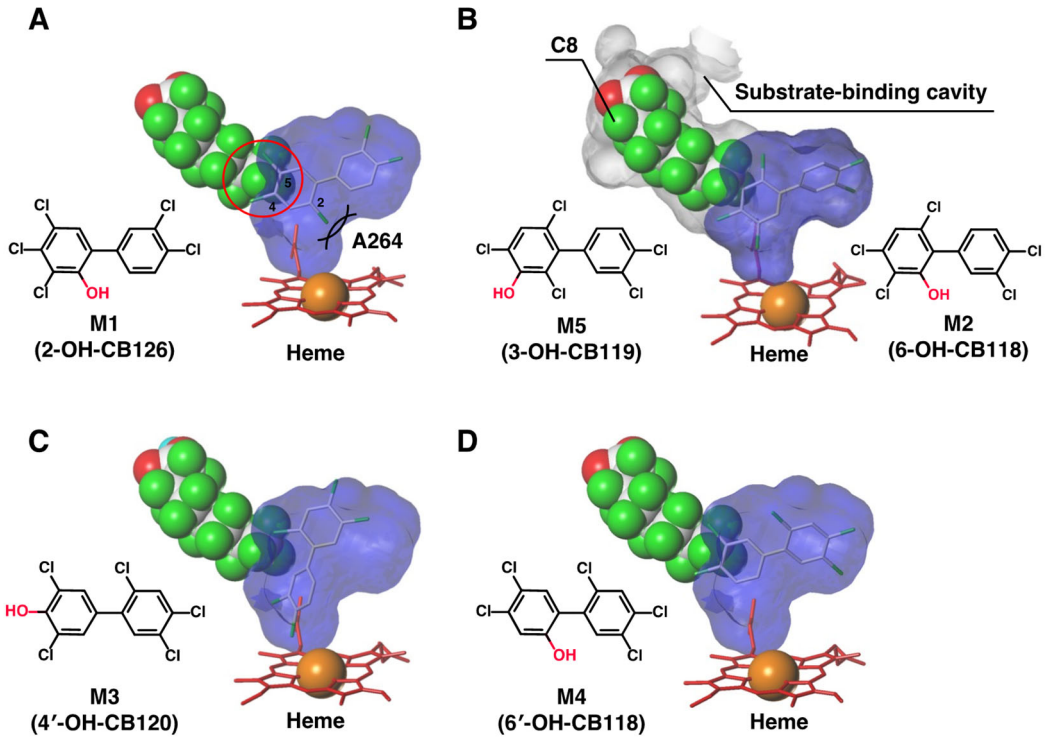

Figure 7 Docking analysis for 2,3′,4,4′,5-pentachlorobiphenyl (CB118) with perfluorooctanoic acid (C8) in the substrate-binding cavity of P450BM3 wild type (WT)

The metabolites M2, M4, and M5 were predicted to be 6-hydroxy (OH)-CB118, 6′-OH-CB118, and 3-OH-2,3′,4,4′,6-pentachlorobiphenyl (3-OH-CB119), respectively. M3 was identified as 4′-OH-2,3′,4,5,5′-pentachlorobiphenyl (4′-OH-CB120) because its retention time index and isotope ratio of M3 were identical to those of S1 (4′-OH-CB120). The P450BM3 WT did not produce metabolite M1 because of the steric hindrance of chlorine atoms at the 2-position to A264, and at the 4- and 5-positions to C8 (red circle). The trichloro (A, B) and dichloro (C, D) rings of CB118 were directed to the heme of the P450BM3 WT in the substrate-binding cavity. M1 is predicted to be 2-OH-3,3′,4,4′,5-pentachlorobiphenyl (2-OH-CB126).

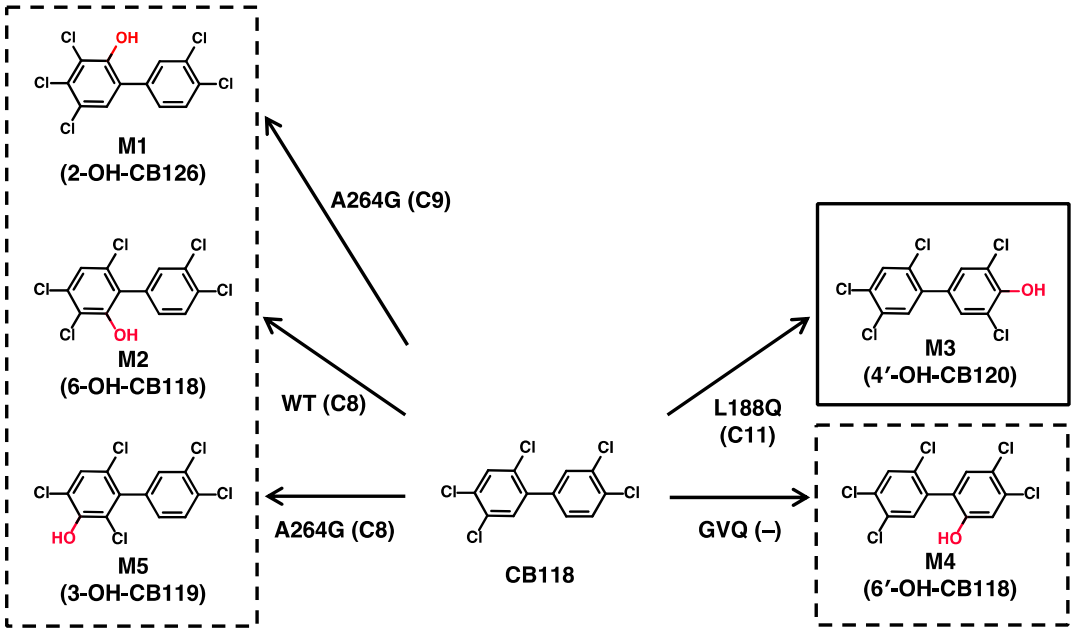

Figure 8 Proposed metabolic pathways for 2,3′,4,4′,5-pentachlorobiphenyl (CB118) with perfluoroalkyl carboxylic acids (PFCAs) by the P450BM3 wild type (WT) and its mutants The solid and dotted boxes represent identified and unidentified metabolites, respectively. The P450BM3 WT and its mutants showing the highest hydroxylation activities are indicated by arrows. The GVQ mutant contained the A74G/F87V/L188Q mutations. The parentheses below the arrows show the PFCAs with the highest hydroxylation activity.

3.6. Conclusions

In this study, we examined the effects of mutations in the WT toward CB118 metabolism. Mutations cause expansion and reduction of the substrate-binding cavity space. These volume changes result in an increase and decrease in reaction activities. Considerably mutation studies using P450BM3 to confer new substrate specificity and enhanced activities have been performed (Whitehouse et al., 2012) because P450BM3 is readily purified from an exogenously expressed host and shows high activity toward various compounds. In a previous study, we reported that WT showed high hydroxylation activity toward CB118 with the assistance of PFCAs (Goto et al.,

2018), while low activity occurred without the addition of PFCAs. This study clarified that the higher activities observed without PFCA were achieved using the L188Q mutation through the induction of the closed form. In contrast, the A264G mutant showed enhanced activity due to increased space above the heme. Furthermore, docking models of P450BM3 mutants and CB118 revealed that the close positions of CB118 to the heme in the conformation with less steric hindrance were hydroxylated. CB118 is predominantly present in estuarine sediments (Hui et al., 2009; Nunes et al., 2011). These mutants are promising for the bioremediation of CB118, even in the absence of complex contamination with PFCAs, because hydroxylated metabolites are less toxic and suitable for further degradation to detoxification. However, membrane permeability of PCBs taken up into bacterial cells should be considered for application if bacteria expressing P450BM3 mutant genes are used for bioremediation.

Funding Sources

This work was conducted in part by the joint research program of the Biosignal Research Center, Kobe University (2016–2020).

Acknowledgements

We thank Prof. Stephen G. Sliger of the University of Illinois for providing the *P450BM3* gene.

We would like to thank Editage (www.editage.com) for the English language editing.

References

Carmichael, A.B., Wong, L.L., 2001. Protein engineering of Bacillus megaterium CYP102: The oxidation of polycyclic aromatic hydrocarbons. Eur. J. Biochem. 268, 3117–3125. https://doi.org/10.1046/j.1432-1327.2001.02212.x.

Dubey, K.D., Wang, B., Shaik, S., 2016. Molecular dynamics and QM/MM calculations predict the substrate-induced gating of cytochrome P450 BM3 and the regio- and stereoselectivity of fatty acid hydroxylation. J. Am. Chem. Soc. 138, 837–845. https://doi.org/10.1021/jacs.5b08737.

Germain, J., Raveton, M., Binet, M.N., Mouhamadou, B., 2021. Screening and metabolic potential of fungal strains isolated from contaminated soil and sediment in the polychlorinated biphenyl degradation. Ecotoxicol. Environ. Saf. 208, 111703. https://doi.org/10.1016/j.ecoenv.2020.111703.

Geronimo, I., Denning, C.A., Heidary, D.K., Glazer, E.C., Payne, C.M., 2018. Molecular determinants of substrate affinity and enzyme activity of a cytochrome P450BM3 variant. Biophys. J. 115, 1251–1263. https://doi.org/10.1016/j.bpj.2018.08.026.

Goto, E., Haga, Y., Kubo, M., Itoh, T., Kasai, C., Shoji, O., Yamamoto, K., Matsumura, C.,

Nakano, T., Inui, H., 2018. Metabolic enhancement of 2,3′,4,4′,5-pentachlorobiphenyl (CB118) using cytochrome P450 monooxygenase isolated from soil bacterium under the presence of perfluorocarboxylic acids (PFCAs) and the structural basis of its metabolism. Chemosphere 210, 376–383. https://doi.org/10.1016/j.chemosphere.2018.07.026.

Hens, B., Hens, L., 2018. Persistent threats by persistent pollutants: Chemical nature, concerns and future policy regarding PCBs—What are we heading for? Toxics 6, 1–21. https://doi.org/10.3390/toxics6010001.

Horváthová, H., Lászlová, K., Dercová, K., 2018. Bioremediation of PCB-contaminated shallow river sediments: The efficacy of biodegradation using individual bacterial strains and their consortia. Chemosphere 193, 270–277. https://doi.org/10.1016/j.chemosphere.2017.11.012.

Hui, Y., Zheng, M., Liu, Z., Gao, L., 2009. PCDD/Fs and dioxin-like PCBs in sediments from Yellow Estuary and Yangtze Estuary, China. Bull. Environ. Contam. Toxicol. 83, 614–619. https://doi.org/10.1007/s00128-009-9832-3.

Inui, H., Itoh, T., Yamamoto, K., Ikushiro, S.-I., Sakaki, T., 2014. Mammalian cytochrome P450-dependent metabolism of polychlorinated dibenzo-*p*-dioxins and coplanar polychlorinated biphenyls. Int. J. Mol. Sci. 15. https://doi.org/10.3390/ijms150814044.

Jing, R., Fusi, S., Kjellerup, B. V, 2018. Remediation of polychlorinated biphenyls (PCBs) in

425 contaminated soils and sediment: State of knowledge and perspectives. Front. Environ.
426 Sci. 6, 79. https://doi.org/10.3389/fenvs.2018.00079
427 Kawakami, N., Shoji, O., Watanabe, Y., 2011. Use of perfluorocarboxylic acids to trick
428 cytochrome P450BM3 into initiating the hydroxylation of gaseous alkanes. Angew.
429 Chemie - Int. Ed. 50, 5315–5318. https://doi.org/10.1002/anie.201007975.
430 Khalid, F., Hashmi, M.Z., Jamil, N., Qadir, A., Ali, M.I., 2021. Microbial and enzymatic
431 degradation of PCBs from e-waste-contaminated sites: a review. Environ. Sci. Pollut. Res.
432 28, 10474–10487. https://doi.org/10.1007/s11356-020-11996-2.
433 Kunisue, T., Tanabe, S., 2009. Hydroxylated polychlorinated biphenyls (OH-PCBs) in the blood
434 of mammals and birds from Japan: Lower chlorinated OH-PCBs and profiles.
435 Chemosphere 74, 950–961. https://doi.org/10.1016/j.chemosphere.2008.10.038.
436 Li, H., Poulos, T.L., 1997. The structure of the cytochrome P450BM-3 haem domain complexed
437 with the fatty acid substrate, palmitoleic acid. Nat. Struct. Biol. 4, 140–146.
438 https://doi.org/10.1038/nsb0297-140
439 Li, Q., Ogawa, J.U.N., Schmid, R.D., Icrobiol, A.P.P.L.E.N.M., 2001. Engineering cytochrome
440 P450 BM-3 for oxidation of polycyclic aromatic hydrocarbons. Appl. Environmental.
441 Microbiol. 67, 5735–5739. https://doi.org/10.1128/AEM.67.12.5735.
442 Mise, S., Haga, Y., Itoh, T., Kato, A., Fukuda, I., Goto, E., Yamamoto, K., Yabu, M.,

443 Matsumura, C., Nakano, T., Sakaki, T., Inui, H., 2016. Structural determinants of the
444 position of 2,3′,4,4′,5-pentachlorobiphenyl (CB118) hydroxylation by mammalian
445 cytochrome P450 monooxygenases. Toxicol. Sci. 152, 340–348.
446 https://doi.org/10.1093/toxsci/kfw086.
447 Narhi, L.O., Fulco, A.J., 1987. Identification and characterization of two functional domains in
448 cytochrome P-450BM-3, a catalytically self-sufficient monooxygenase induced by
449 barbiturates in Bacillus megaterium. J. Biol. Chem. 262, 6683–6690.
450 https://doi.org/10.1016/s0021-9258(18)48296-8.
451 Nunes, M., Marchand, P., Vernisseau, A., Bizec, B. Le, Ramos, F., Pardal, M.A., 2011.
452 PCDD/Fs and dioxin-like PCBs in sediment and biota from the Mondego estuary
453 (Portugal). Chemosphere 83, 1345–1352.
454 https://doi.org/10.1016/j.chemosphere.2011.02.081.
455 Ohkawa, H., Inui, H., 2015. Metabolism of agrochemicals and related environmental chemicals
456 based on cytochrome P450s in mammals and plants. Pest Manag. Sci. 71, 824–828.
457 https://doi.org/10.1002/ps.3871.
458 Omura, T., Sato, R., 1964. The carbon monoxide-binding pigment of liver microsomes: I.
459 evidence for its hemoprotein nature. J. Biol. Chem. 239, 2370–2378.
460 https://doi.org/10.1016/S0021-9258(20)82244-3.

461 Ruppert, J., Welch, W., Jain, A.N., 1997. Automatic identification and representation of protein
462 binding sites for molecular docking. Protein Sci. 6, 524–533.
463 https://doi.org/10.1002/pro.5560060302.
464 Sulistyaningdyah, W.T., Ogawa, J., Li, Q.S., Shinkyo, R., Sakaki, T., Inouye, K., Schmid, R.D.,
465 Shimizu, S., 2004. Metabolism of polychlorinated dibenzo-*p*-dioxins by cytochrome
466 P450BM-3 and its mutant. Biotechnol. Lett. 26, 1857–1860.
467 https://doi.org/10.1007/s10529-004-5317-y.
468 Suzuki, K., Stanfield, J.K., Omura, K., Shisaka, Y., Ariyasu, S., Kasai, C., Aiba, Y., Sugimoto,
469 H., Shoji, O., 2023. A compound I mimic reveals the transient active species of a
470 cytochrome P450 enzyme: Insight into the stereoselectivity of P450-catalysed oxidations.
471 Angew. Chemie - Int. Ed. e202215706. https://doi.org/10.1002/anie.202215706.
472 Weber, R., Herold, C., Hollert, H., Kamphues, J., Blepp, M., Ballschmiter, K., 2018. Reviewing
473 the relevance of dioxin and PCB sources for food from animal origin and the need for
474 their inventory, control and management. Environ. Sci. Eur. 30, 42.
475 https://doi.org/10.1186/s12302-018-0166-9.
476 Whitehouse, C.J.C., Bell, S.G., Wong, L.-L., 2012. P450 $_{BM3}$ (CYP102A1): connecting the dots.
477 Chem. Soc. Rev. 41, 1218–1260. https://doi.org/10.1039/C1CS15192D.
478 Xiang, Y., Xing, Z., Liu, J., Qin, W., Huang, X., 2020. Recent advances in the biodegradation

of polychlorinated biphenyls. World J. Microbiol. Biotechnol. 36, 1–10. https://doi.org/10.1007/s11274-020-02922-2.

Yabu, M., Haga, Y., Itoh, T., Goto, E., Suzuki, M., Yamazaki, K., Mise, S., Yamamoto, K., Matsumura, C., Nakano, T., Sakaki, T., Inui, H., 2022. Hydroxylation and dechlorination of 3,3′,4,4′-tetrachlorobiphenyl (CB77) by rat and human CYP1A1s and critical roles of amino acids composing their substrate-binding cavity. Sci. Total Environ. 837, 155848. https://doi.org/10.1016/j.scitotenv.2022.155848.

Yamazaki, K., Suzuki, M., Itoh, T., Yamamoto, K., Kanemitsu, M., Matsumura, C., Nakano, T., Sakaki, T., Fukami, Y., Imaishi, H., Inui, H., 2011. Structural basis of species differences between human and experimental animal CYP1A1s in metabolism of 3,3′,4,4′,5-pentachlorobiphenyl. J. Biochem. 149, 487–494. https://doi.org/10.1093/jb/mvr009.

Zhu, M., Yuan, Y., Yin, H., Guo, Z., Wei, X., Qi, X., Liu, H., Dang, Z., 2022. Environmental contamination and human exposure of polychlorinated biphenyls (PCBs) in China: A review. Sci. Total Environ. 805, 150270. https://doi.org/10.1016/j.scitotenv.2021.150270.

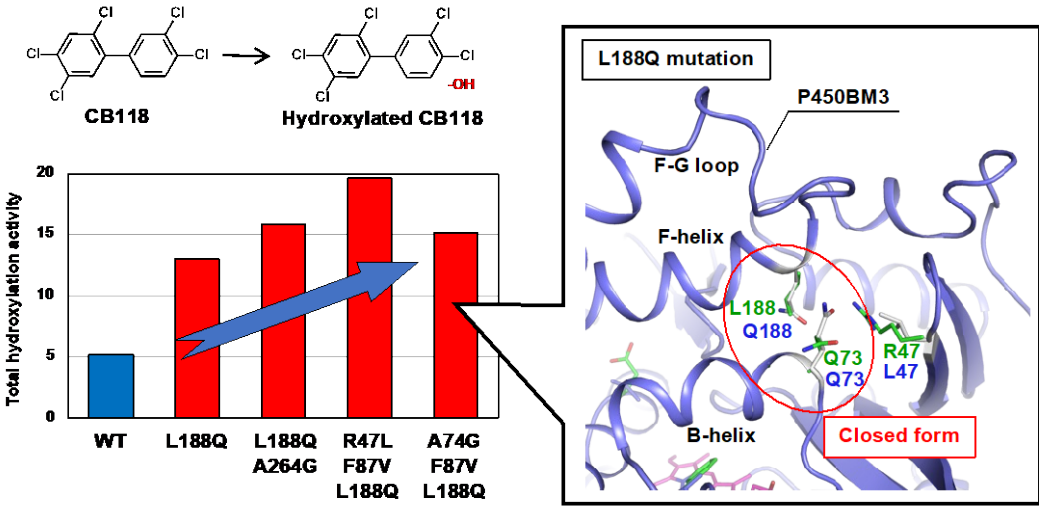

Graphical abstract